

This article was presented at the LII Scientific and Educational Conference of ITMO University, January 31 – February 03, 2023, St. Petersburg, Russia

# Structural Properties of $\beta$ -Ga<sub>2</sub>O<sub>3</sub> Thin Films Obtained on Different Substrates by Sol-Gel Method

M.K. Vronskii<sup>1,\*</sup>, A.Yu. Ivanov<sup>1</sup>, L.A. Sokura<sup>1,2</sup>, A.V. Kremleva<sup>1</sup>, D.A. Bauman<sup>1</sup>

<sup>1</sup> Institute of Advanced Data Transfer Systems, ITMO University, Kronverkskiy pr., 49, lit. A, St. Petersburg, 197101, Russia

<sup>2</sup> Ioffe Institute, Politekhnicheskaya st., 26, St. Petersburg, 194021, Russia

---

## Article history

Received March 10, 2023  
Received in revised form  
March 26, 2023  
Accepted March 27, 2023  
Available online March 31, 2023

## Abstract

$\beta$ -Ga<sub>2</sub>O<sub>3</sub> thin films were obtained by the sol-gel method on sapphire and quartz substrates, as well as on Cu-O buffer layers. It was shown that the sol-gel method allowed to obtain  $\beta$ -Ga<sub>2</sub>O<sub>3</sub> thin films with good optical and structural properties by using X-ray diffraction, scanning electron microscopy and optical spectroscopy. The energy of the optical band gap of Ga<sub>2</sub>O<sub>3</sub> films calculated by the Tauc plot varied from 4.39 to 4.59 eV.

---

*Keywords:*  $\beta$ -Ga<sub>2</sub>O<sub>3</sub>; UWB semiconductor; XRD; Thin film; Sol-gel

## 1. INTRODUCTION

Ultra-wide bandgap (UWBG) semiconductors have such distinctive advantages as thermodynamic stability and high breakdown voltage. Due to these properties, such materials can be used in power electronics and in various optoelectronic devices, including ultraviolet “solar-blind” photodetectors, gas-sensitive devices, thin-film transistors and Schottky barrier diodes [1–4].

At present, diamond (with band gap of 5.5 eV), aluminum gallium nitride AlGa<sub>N</sub> (3.4–6.2 eV) and  $\beta$ -phase gallium oxide  $\beta$ -Ga<sub>2</sub>O<sub>3</sub> (4.8–4.9 eV) are the most perspective UWBG semiconductor materials [5]. Among them, Ga<sub>2</sub>O<sub>3</sub> is the most promising material for use in power electronics of a new generation, assuming operation at high voltages and temperatures.

It is known that gallium oxide can crystallize in 5 (or 6 according to some studies) different crystalline phases [6], but the  $\beta$ -phase of Ga<sub>2</sub>O<sub>3</sub> is of the greatest interest not only due to its wide band gap of 4.8–4.9 eV, but also its high thermodynamic stability [6,7].

By now, thin films of  $\beta$ -Ga<sub>2</sub>O<sub>3</sub> have been obtained by various epitaxial methods, including molecular beam epitaxy [8–11], metalorganic [12–15] and hydride vapor-phase epitaxy [16–18], and non-epitaxial methods — chemical deposition from the low-pressure vapor phase [19–21] and sol-gel method [22–25].

The sol-gel method can significantly reduce the cost of manufacturing thin films compared to epitaxial methods [26]. However, the use of sol-gel technology to obtain  $\beta$ -Ga<sub>2</sub>O<sub>3</sub> is insufficiently studied and requires additional research to improve the structural state of the resulting thin films.

In this study,  $\beta$ -Ga<sub>2</sub>O<sub>3</sub> thin films were obtained by the sol-gel method in various technological parameters such as the substrate material, the presence and thickness of copper oxide buffer layers, as well as the mode of high-temperature processing. The comparison of optical and structural properties of films obtained under various conditions was carried out, and the dependence of their properties on the conditions of obtaining was revealed.

---

\* Corresponding author: M.K. Vronskii, e-mail: [mkvronskii@itmo.ru](mailto:mkvronskii@itmo.ru)

## 2. METHODS

To obtain the Ga<sub>2</sub>O<sub>3</sub> thin films by sol-gel method the gallium nitrate hydrate Ga(NO<sub>3</sub>)<sub>3</sub>·8H<sub>2</sub>O was dissolved in ethyl alcohol (C<sub>2</sub>H<sub>6</sub>O) with the molar concentration of 0.5 M. The catalyst of the reaction was monoethanolamine (MEA, C<sub>2</sub>H<sub>7</sub>NO). MEA was added to the solution in a ratio of 1:1 to Ga after complete dissolution of gallium nitrate in ethanol. The resulting solution was stirred for 90 minutes at a temperature of 60 °C.

Plates of fused quartz and sapphire with a diameter of 20 mm and a thickness of 1 mm were used as a substrate. To improve the adhesion of the films, the substrates were previously cleaned in an ultrasonic bath in acetone, ethyl alcohol and deionized water sequentially for 10 minutes.

Buffer layers of copper oxide were obtained on quartz and sapphire substrates by deposition of copper layer by magnetron sputtering in vacuum using the Q150R plus (Quorum) and further annealing at 200 °C for 1.5 hours. XRD study showed that the film obtained in that way contained CuO and Cu<sub>2</sub>O phases.

Gallium oxide layers were made by the spin coating method. The solution was coated at a speed of 3000 rpm for 30 seconds. Then samples were dried in the air at a temperature of 100 °C for 10 minutes and were pre-annealed at a temperature of 500 °C in the air for 15 minutes. The drying temperature (100 °C) was chosen in such a way as to evaporate the sol solvent without boiling. The temperature of the intermediate annealing (500 °C) was chosen to obtain primary crystallization from the gallium hydroxyl and other phases of the Ga-O system into the  $\alpha$ - and  $\beta$ -phases of gallium oxide [27]. The procedure of layers coating, drying and annealing was repeated 6 times to increase the total thickness of the film.

After all the stages of layers coating and drying, the final annealing was carried out at a temperature of 900 °C in the air for 4 hours to recrystallize the intermediate phases to the  $\beta$ -Ga<sub>2</sub>O<sub>3</sub>. Thus, six films samples series were obtained by the sol-gel method with various technological parameters, their description is given in Table 1. After the structural investigation of obtained films, the samples were annealed once again for 2 hours at a temperature of 1100 °C, and the studies were repeated.

To study the phase composition and crystal structure of the obtained films, the X-ray diffraction analysis (XRD) was used on DRON-8 (Bourestnik) installation in the wide-slit configuration with a fine focus BSV-29 tube with a copper anode and NaI (Tl) scintillation detector. The XRD patterns of samples were recorded during scanning in the angular range  $2\theta = 10^\circ$ – $70^\circ$  at a step of  $\Delta(2\theta) = 0.05^\circ$  and a rotation speed of 30 rpm.

Structure and thickness of the obtained films were studied by scanning electron microscopy (SEM) using

**Table 1.** Parameters of obtained  $\beta$ -Ga<sub>2</sub>O<sub>3</sub> thin films.

Sample name	Buffer layer/Substrate	Buffer layer thickness, nm
A	–/Al <sub>2</sub> O <sub>3</sub>	–
B	–/SiO <sub>2</sub>	–
C	Cu-O/SiO <sub>2</sub>	120
D	Cu-O/Al <sub>2</sub> O <sub>3</sub>	120
E	Cu-O/SiO <sub>2</sub>	240
F	Cu-O/Al <sub>2</sub> O <sub>3</sub>	240

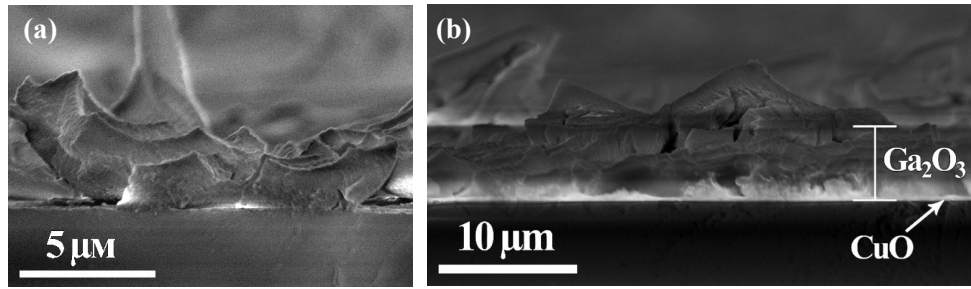
Mira-3 (Tescan). To determine the film thickness by SEM the samples were prepared in the cross-sectional geometry by mechanically chipping in a direction normal to the surface plane.

The optical properties of the samples were determined by Avantes fiber-optic spectroscopy system consisting of Avaspec-2048 spectrometer and Ava-Light D(H)-S deuterium-halogen light source allowing measurement of the absorption and transmission spectra of samples in the range of 200–1100 nm. By using AvaSpec spectrometer and AvaSoft software, the samples absorption was measured according to the Booger-Lambert-Beer law.

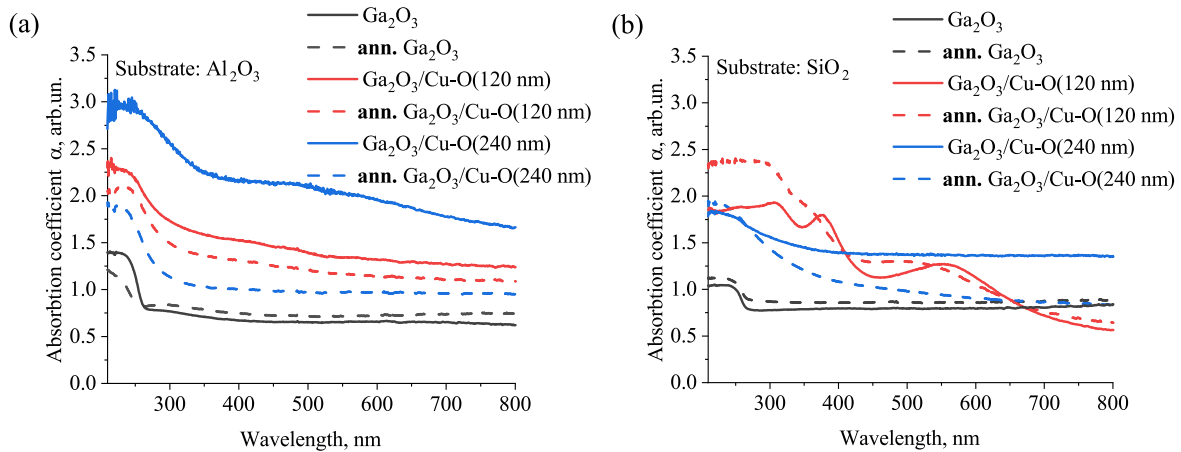
## 3. RESULTS AND DISCUSSION

Fig. 1 shows the SEM images of samples A and D with gallium oxide films obtained on sapphire substrates without and with a copper oxide buffer layer, respectively. All samples showed a pronounced heterogeneity of the surface. Fig. 1a shows the film in the sample A consists of separate fragments of several micrometers in size, and the average thickness of film was 1.6 micrometers. A similar film structure was observed for samples obtained on a quartz substrate. However, the use of a Cu-O buffer layer allows to obtain a continuous film on the substrate surface (Fig. 1b; sample D). The average thickness of such film was 6 micrometers, but protruding fragments of 3–5 micrometers in size were observed on its surface. The thickness of the films differed for samples on copper oxide layer and without it. Several factors can probably contribute to an increase in film thickness: different adhesion of sol to substrates during spin-coating of layers, different density of the obtained films and different degree of crystallization, which is the result, for example, of different heat capacity of the substrates, which may affect the annealing process.

Fig. 2 shows the absorption spectra of A–D samples in the range of 215–800 nm. These spectra contain the absorption edge of the gallium oxide films for samples A and B which are clearly observed about 270 nm. The absorption



**Fig. 1.** SEM images of cross section of (a)  $\text{Ga}_2\text{O}_3/\text{Al}_2\text{O}_3$  (sample A) and (b)  $\text{Ga}_2\text{O}_3/\text{Cu-O}/\text{Al}_2\text{O}_3$  (sample D) films.



**Fig. 2.** Absorption spectra of gallium oxide films obtained on the sapphire (a) and fused quartz (b) substrates: the black curve corresponds to the spectra for the gallium oxide layer without the copper oxide buffer layer, the red curve corresponds to a heterostructure with a copper oxide buffer layer of 120 nm thickness, the blue curve corresponds to a heterostructure with a copper oxide buffer layer of 240 nm thickness. Dashed curves indicate the absorption spectra of films with additional annealing at a temperature of 1100 °C.

coefficient of a film obtained on a sapphire substrate significantly exceeds the absorption coefficient of a film obtained on a quartz substrate. Since their thickness is approximately the same (1.6–2 μm), it is probably due to the different crystal quality of the obtained films [28].

A comparison of the absorption spectra in Fig. 2 shows that the use of a copper oxide buffer layer has significantly increased the absorption of gallium oxide in the UV region, but at the same time samples sharp absorption edge became smoother. An increase in the buffer layer thickness from 120 nm to 240 nm allowed the additional increase and smoothing in the absorption spectra. Also, with an increase in the thickness of the copper oxide buffer layer the energy shift of the absorption edge occurred towards a lower energy (longer wavelength).

An interesting fact is that additional annealing allowed a decrease in the intensity of absorption spectra of films on sapphire substrate compared to samples before it. After additional annealing the absorption edge of the sample with a thin copper oxide buffer layer (120 nm) remained virtually unchanged. But for sample with a thick copper oxide buffer layer (240 nm) the inclination angle of absorption edge increased, which made the absorption edge

more similar to the absorption edge of gallium oxide film without copper oxide.

Surprisingly, the absorption spectra for samples on the fused quartz substrates show different dependences at an increase in the thickness of the copper oxide buffer layer and after additional annealing. An additional annealing, however, led to a slight increase in absorption for samples without copper oxide layer and with a thick copper oxide layer (240 nm) in the UV range. Sample with a thin copper oxide layer (120 nm) significantly increased the absorption in the UV range after additional annealing.

Fig. 3 shows the dependence of the absorption coefficient for the substrates and substrates with copper oxide layer. As can be seen, the used substrates had a low absorption over the entire spectral range under study. The addition of copper oxide layer increased absorption in the UV range and in the optical region closer to UV. It can be also seen that the absorption is higher for quartz substrate with the copper oxide layer than for sapphire with copper oxide.

A comparison of the absorption spectra in Figs. 2 and 3 shows that absorption coefficient for  $\text{Ga}_2\text{O}_3/\text{Cu-O}/\text{SiO}_2$  structures is lower than that for  $\text{Cu-O}/\text{SiO}_2$  structure. After

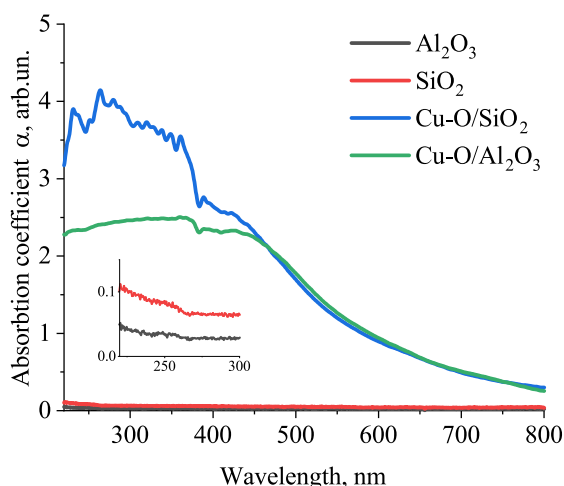


**Fig. 3.** The absorption coefficient of substrates and the substrates with copper oxide buffer layer. These dependences were obtained before the coating of gallium oxide layer to these substrates. The insert shows that the absorption of sapphire and quartz substrates are similar in visible spectra and substrates begin to absorb in the wavelength range of UV-C.

coating of gallium oxide onto the copper oxide layer, these layers were annealed together at high temperature. It is probably that during this annealing, in addition to the crystallization of gallium oxide, the recrystallization of copper oxide also occurred, which led to an improvement in its optical properties. Actually, looking forward, the improvement of the crystalline properties of copper oxide layers as a result of annealing was also observed on the X-ray diffractogram.

Analysis of the absorption spectra in the Tauc plot [29] allowed to see that the absorption edge shifts with an increase in the thickness of the copper oxide buffer layer.

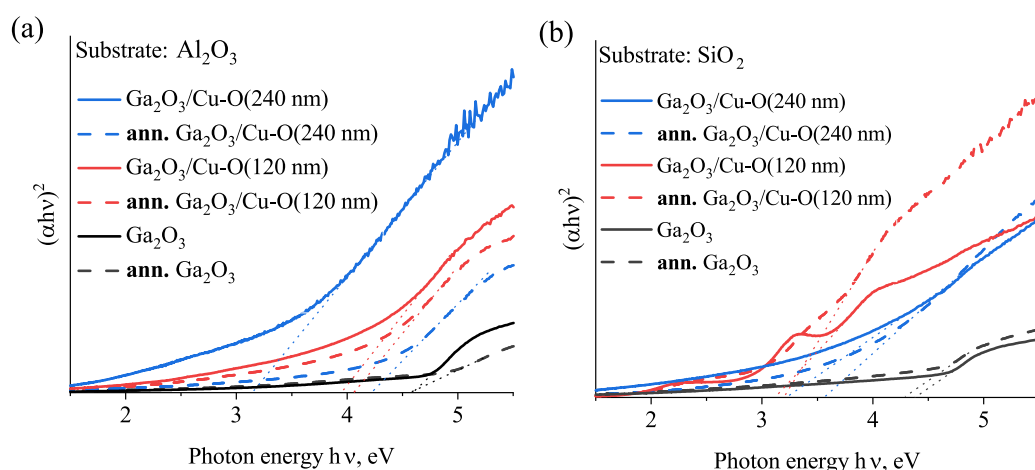


**Fig. 4.** Tauc plot of absorption coefficient spectra of gallium oxide films obtained on the sapphire (a) and fused quartz (b) substrates: the black curve corresponds to the spectra for the gallium oxide layer without the copper oxide buffer layer, the red curve corresponds to a heterostructure with a copper oxide buffer layer of 120 nm thickness, the blue curve corresponds to a heterostructure with a copper oxide buffer layer of 240 nm thickness. Dashed curves indicate the absorption spectra of films with additional annealing at a temperature of 1100 °C. Straight dotted lines are approximation curves constructed by the Tauc method, showing the absorption edges for the studied films.

For gallium oxide film on the sapphire substrate the value of absorption edge before annealing and after annealing was the same (approximately 4.59 eV) [30–32]. In the presence of thin copper oxide layer (120 nm) the annealing led to a decrease in the wavelength and, accordingly, an increase in the energy of the absorption edge from 3.94 eV to 4.09 eV. In the presence of thick copper oxide layer (240 nm) the annealing also led to an increase in the energy of the absorption edge from 3.21 eV to 4.31 eV showing better crystallization of gallium oxide film.

For samples on the quartz substrate, the annealing led to a decrease of the absorption edge for gallium oxide from 4.42 eV to 4.25 eV. The addition of thin copper oxide layer (120 nm) led to decrease in the absorption edge energy to 3.14–3.18 eV for samples before and after annealing. An increase in the copper oxide layer thickness up to 240 nm led to an increase in the absorption edge to 3.25–3.55 eV.

Fig. 5 shows XRD patterns of the samples A–D. All patterns had many reflections peaks corresponding to the monoclinic crystal lattice of the  $\beta$ -phase of gallium oxide. The low intensity of reflections (Figs. 5a,b) indicated incomplete crystallization of the films. Probably, the resulting films have a polycrystalline structure with a small crystallite size, as was observed during the SEM studies (Fig. 1). To confirm this, an additional annealing at temperature 1100 °C for 2 hours was carried out. This slightly improved the crystalline quality of the films, which contributed to an increase in reflections intensity on diffractograms (Figs. 5c,d) and led to the appearance of more reflections from Cu-O compounds.

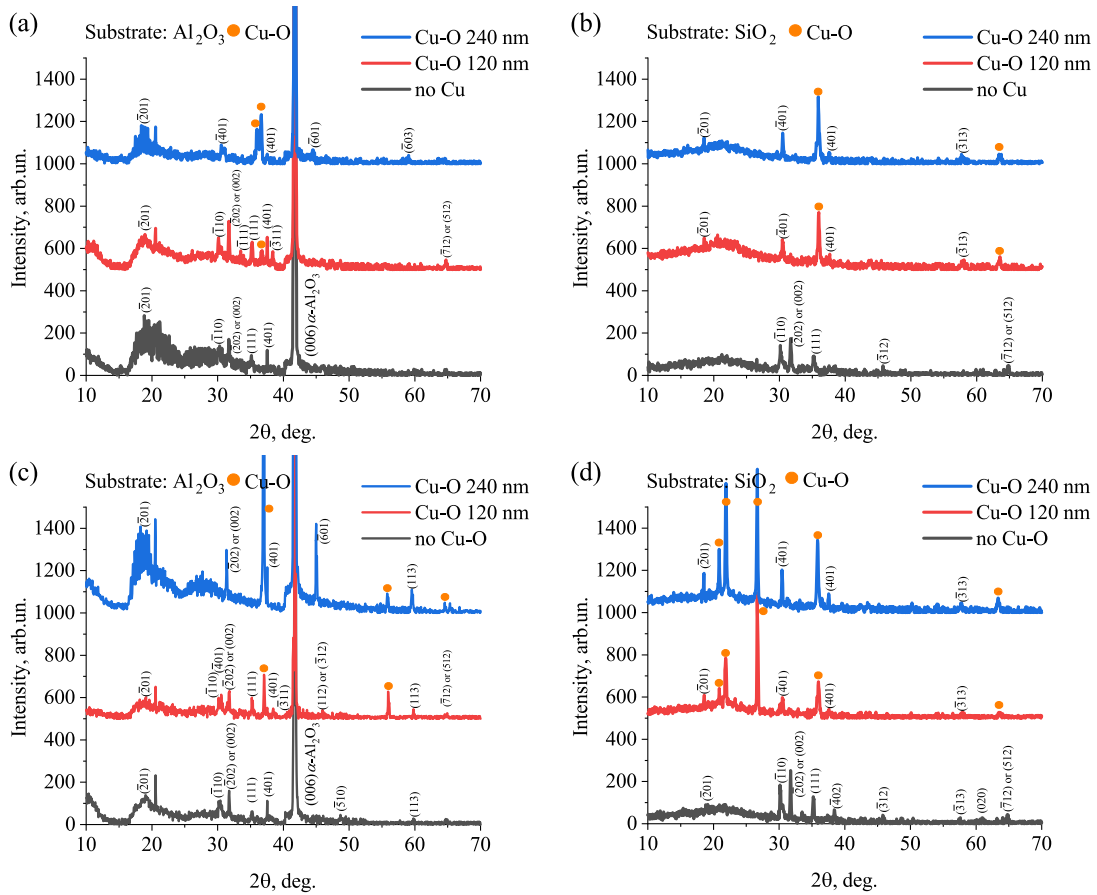


**Fig. 5.** XRD patterns of obtained films  $\text{Ga}_2\text{O}_3$  on  $\text{Al}_2\text{O}_3$  and  $\text{SiO}_2$  substrates. Subfigures (a) and (b) corresponds to the XRD patterns obtained after the first annealing, (c) and (d) corresponds to a heterostructure after the additional annealing. The black curve corresponds to the samples without using a copper oxide buffer layer. The red curve and blue curve mark samples with a buffer layer with thickness of 120 nm and 240 nm, respectively.

Comparing the peaks intensity of diffractograms, it can be seen that for a gallium oxide film obtained on a sapphire substrate without copper oxide buffer layer, the increase in intensity after annealing was 43% bigger relative to the noise intensity level. The addition of a copper oxide layer made it possible to increase the peaks intensity and to get fewer reflections from different planes, which may indicate an increase in the number of grains or crystallites in the films. The intensity of reflections for a sample with 240 nm Cu-O layer thickness increased by about 52% after annealing.

In addition to the fact that the number of reflections on diffractograms has increased after annealing, it can be seen that their intensity has increased and the amount of amorphous component on diffractograms has decreased (Fig. 5). This effect is especially noticeable on samples without copper oxide buffer layer and with a thin copper oxide layer. But this effect is not observed on a sample with a thick layer of copper oxide on sapphire substrate. Comparison of the XRD patterns showed that the films obtained on the buffer layer of copper oxide had better crystal quality (Figs. 5a,b), which was also observed in SEM studies. Probably, the better crystal quality contributed to the

lower absorption of films in the visible range 300–800 nm, which was observed earlier (Fig. 2). An increase in the thickness of the copper oxide buffer layer from 120 nm to 240 nm led to an increase in the intensity of gallium oxide reflections in diffraction patterns, and, probably, to an improvement in the crystal quality of the samples.

#### 4. CONCLUSION

Thin films of  $\beta\text{-Ga}_2\text{O}_3$  were obtained by the sol-gel method on quartz and sapphire substrates, and Cu-O buffer layers. The influence of the substrate material, the presence and thickness of copper oxide buffer layers and the annealing temperature on their crystal quality was studied. Optical transitions, probably associated with interband absorption, were detected in the range of 270–330 nm (from 3.70 to 4.59 eV). It was also found that the films had a polycrystalline structure and high surface heterogeneity, and their thickness was from 1.6 to 6  $\mu\text{m}$ . The use of a sapphire substrate, buffer layers of copper oxide of large thickness (240 nm) and additional annealing at 1100  $^\circ\text{C}$  made it possible to improve the crystal quality of the resulting thin films of  $\beta\text{-Ga}_2\text{O}_3$ .

## ACKNOWLEDGEMENTS

The study was carried out within the framework of the research program of the scientific school “Theory and practice of advanced materials and devices of optoelectronics and electronics” (sci. school 5082.2022.4).

The authors are grateful to A. M. Smirnov for constructive comments and substantial discussions of the results of this study.

## REFERENCES

- [1] O. Sooyeon, Y. Gwangseok, K. Jihyun, *Electrical Characteristics of Vertical Ni/ $\beta$ -Ga<sub>2</sub>O<sub>3</sub> Schottky Barrier Diodes at High Temperatures*, ECS Journal of Solid State Science and Technology, 2017, vol. 6, no. 2, pp. Q3022–Q3025.
- [2] S.R.Thomas, G. Adamopoulos, Y.–H. Lin, H. Faber, L. Sygellou, E. Stratakis, N. Pliatsikas, P.A. Patsalas, T.D. Anthopoulos, *High Electron Mobility Thin–Film Transistors Based on Ga<sub>2</sub>O<sub>3</sub> Grown by Atmospheric Ultrasonic Spray Pyrolysis at Low Temperatures*, Applied Physics Letters, 2014, vol. 105, no. 9, art. no. 092105.
- [3] A.Yu. Ivanov, A.V. Kremleva, Sh.Sh. Sharofidinov, *The Electrical Properties of Schottky Barrier Diode Structures Based on HVPE Grown Sn Doped Ga<sub>2</sub>O<sub>3</sub> Layers*, Reviews on Advanced Materials and Technologies, 2022, vol. 4, no. 1, pp. 33–38.
- [4] M.A. Rozhkov, E.S. Kolodeznyi, A.M. Smirnov, V.E. Bougrov, A.E. Romanov, *Comparison of characteristics of Schottky diode based on  $\beta$ -Ga<sub>2</sub>O<sub>3</sub> and other wide bandgap semiconductors*, Materials Physics and Mechanics, 2015, vol. 24, no. 2, pp. 194–200.
- [5] P.J.Wellmann, *Power electronic semiconductor materials for automotive and energy saving applications–SiC, GaN, Ga<sub>2</sub>O<sub>3</sub>, and diamond*, Zeitschrift für anorganische und allgemeine Chemie, 2017, vol. 643 no. 21, pp. 1312–1322.
- [6] S. Yoshioka, H. Hayashi, A. Kuwabara, F. Oba, K. Matsunaga, I. Tanaka, *Structures and energetics of Ga<sub>2</sub>O<sub>3</sub> polymorphs*. Journal of Physics: Condensed Matter, 2007, vol. 19 no. 34, art. no. 346211.
- [7] N. Ueda, H. Hosono, R. Waseda, H. Kawazoe, *Synthesis and control of conductivity of ultraviolet transmitting  $\beta$ -Ga<sub>2</sub>O<sub>3</sub> single crystals*, Applied Physics Letters, 1997, vol. 70, no. 26, pp. 3561–3563.
- [8] E.G. Villora, K. Shimamura, K. Kitamura, K. Aoki, *Rf-plasma-assisted molecular-beam epitaxy of  $\beta$ -Ga<sub>2</sub>O<sub>3</sub>*, Applied Physics Letters, 2006, vol. 88, no. 3, art. no. 031105.
- [9] K. Sasaki, A. Kuramata, T. Masui, E.G. Villora, K. Shimamura, S. Yamakoshi, *Device-quality  $\beta$ -Ga<sub>2</sub>O<sub>3</sub> epitaxial films fabricated by ozone molecular beam epitaxy*, Applied Physics Express, 2012, vol. 5, no. 3, art. no. 035502.
- [10] K. Sasaki, M. Higashiwaki, A. Kuramata, T. Masui, S. Yamakoshi, *Growth temperature dependences of structural and electrical properties of Ga<sub>2</sub>O<sub>3</sub> epitaxial films grown on  $\beta$ -Ga<sub>2</sub>O<sub>3</sub> (010) substrates by molecular beam epitaxy*, Journal of Crystal Growth, 2014, vol. 392, pp. 30–33.
- [11] D. Guo, Z. Wu, P. Li, Y. An, H. Liu, X. Guo, H. Yan, G. Wang, C. Sun, L. Li, W. Tang, *Fabrication of  $\beta$ -Ga<sub>2</sub>O<sub>3</sub> thin films and solar-blind photodetectors by laser MBE technology*, Optical Materials Express, 2014, vol. 4, no. 5, pp. 1067–1076.
- [12] N.H. Kim, H.W. Kim, C. Lee, *Amorphous gallium oxide nanowires synthesized by metalorganic chemical vapor deposition*, Materials Science and Engineering: B, 2004, vol. 111, no. 2–3, pp. 131–134.
- [13] H.W. Kim, N.H. Kim, *Growth of gallium oxide thin films on silicon by the metal organic chemical vapor deposition method*, Materials Science and Engineering: B, 2004, vol. 110, no. 1, pp. 34–37.
- [14] G. Wagner, M. Baldini, D. Gogova, M. Schmidbauer, R. Schewski, M. Albrecht, Z. Galazka, D. Klimm, R. Fornari, *Homoepitaxial growth of  $\beta$ -Ga<sub>2</sub>O<sub>3</sub> layers by metal-organic vapor phase epitaxy*, Physica Status Solidi (a), 2014, vol. 211, no. 1, pp. 27–33.
- [15] M. Baldini, M. Albrecht, A. Fiedler, K. Irmscher, R. Schewski, G. Wagner, *Si- and Sn-doped homoepitaxial  $\beta$ -Ga<sub>2</sub>O<sub>3</sub> layers grown by MOVPE on (010)-oriented substrates*, ECS Journal of Solid State Science and Technology, 2016, vol. 6, no. 2, pp. Q3040–3044.
- [16] K. Nomura, K. Goto, R. Togashi, H. Murakami, Y. Kumagai, A. Kuramata, S. Yamakoshi, A. Koukitu, *Thermodynamic study of  $\beta$ -Ga<sub>2</sub>O<sub>3</sub> growth by halide vapor phase epitaxy*, Journal of Crystal Growth, 2014, vol. 405, pp. 19–22.
- [17] A.V. Kremleva, Sh.Sh. Sharofidinov, A.M. Smirnov, E. Podlesnov, M.V. Dorogov, M.A. Odnoblyudov, V.E. Bougrov, A.E. Romanov, *Growth of thick gallium oxide on the various substrates by halide vapor phase epitaxy*, Materials Physics and Mechanics, 2020, vol. 44, no. 2, pp. 164–171.
- [18] A.M. Smirnov, A.V. Kremleva, A.Yu. Ivanov, A.V. Myasoedov, L.A. Sokura, D.A. Kirilenko, Sh.Sh. Sharofidinov, A.E. Romanov, *Stress–strain state and piezoelectric polarization in orthorhombic Ga<sub>2</sub>O<sub>3</sub> thin films depending on growth orientation*, Materials & Design, 2023, vol. 226, art. no. 111616.
- [19] S. Rafique, L. Han, H. Zhao, *Synthesis of wide bandgap Ga<sub>2</sub>O<sub>3</sub> (E<sub>g</sub>~4.6–4.7 eV) thin films on sapphire by low pressure chemical vapor deposition*, Physica Status Solidi (a), 2016, vol. 213, no. 4, pp. 1002–1009.
- [20] S. Rafique, L. Han, M.J. Tadjer, J.A. Freitas Jr., N.A. Mahadik, H. Zhao, *Homoepitaxial growth of  $\beta$ -Ga<sub>2</sub>O<sub>3</sub> thin films by low pressure chemical vapor deposition*, Applied Physics Letters, 2016, vol. 108, no. 18, art. no. 182105.
- [21] S. Rafique, L. Han, A.T. Neal, S. Mou, M.J. Tadjer, R.H. French, H. Zhao, *Heteroepitaxy of N-type  $\beta$ -Ga<sub>2</sub>O<sub>3</sub> thin films on sapphire substrate by low pressure chemical vapor deposition*, Applied Physics Letters, 2016, vol. 109, no. 13, art. no. 132103.
- [22] M. Yu, C. Lv, J. Yu, Y. Shen, L. Yuan, J. Hu, S. Zhang, H. Cheng, Y. Zhang, R. Jia, *High-performance photodetector based on sol–gel epitaxially grown  $\alpha/\beta$  Ga<sub>2</sub>O<sub>3</sub> thin films*, Materials Today Communications, 2020, vol. 25, art. no. 101532.
- [23] H. Shen, Y. Yin, K. Tian, K. Baskaran, L. Duan, X. Zhao, A. Tiwari, *Growth and characterization of  $\beta$ -Ga<sub>2</sub>O<sub>3</sub> thin films by sol-gel method for fast-response solar-blind ultraviolet photodetectors*, Journal of Alloys and Compounds, 2018, vol. 766, pp. 601–608.
- [24] M.S. Bae, S.H. Kim, J.S. Baek, J.H. Koh, *Comparative study of high–temperature annealed and RTA process  $\beta$ -Ga<sub>2</sub>O<sub>3</sub> thin film by sol–gel process*, Coatings, 2021, vol. 11, no. 10, art. no. 1220.

- [25] M.R. Mohammadi, D.J. Fray, *Semiconductor TiO<sub>2</sub>-Ga<sub>2</sub>O<sub>3</sub> thin film gas sensors derived from particulate sol-gel route*, Acta Materialia, 2007, vol. 55, no. 13, pp. 4455–4466.
- [26] S.S. Park, J.D. Mackenzie, *Sol-gel-derived tin oxide thin films*, Thin Solid Films, 1995, vol. 258, no. 1–2, pp. 268–273.
- [27] H.Y. Playford, A.C. Hannon, E.R. Barney, R.I. Walton, *Structures of uncharacterized polymorphs of gallium oxide from total neutron diffraction*, Chemistry—A European Journal, 2013, vol. 19, no. 8, pp. 2803–2813.
- [28] Y.C. Liu, S.K. Tung, J.H. Hsieh, *Influence of annealing on optical properties and surface structure of ZnO thin films*, Journal of Crystal Growth, 2006, vol. 287, no. 1, pp. 105–111.
- [29] J. Tauc, *Optical properties and electronic structure of amorphous Ge and Si*, Materials Research Bulletin, 1968, vol. 3, no. 1, pp. 37–46.
- [30] M.A. Mastro, A. Kuramata, J. Calkins, J. Kim, F. Ren, S. J. Pearton, *Perspective—opportunities and future directions for Ga<sub>2</sub>O<sub>3</sub>*, ECS Journal of Solid State Science and Technology, 2017, vol. 6, no. 5, pp. P356–P359.
- [31] S.J. Pearton, J. Yang, P.H. Cary IV, F. Ren, J. Kim, M.J. Tadjer, M.A. Mastro, *A review of Ga<sub>2</sub>O<sub>3</sub> materials, processing, and devices*, Applied Physics Reviews, 2018, vol. 5, no. 1, art. no. 011301.
- [32] M. Higashiwaki, G.H. Jessen, *Guest Editorial: The dawn of gallium oxide microelectronics*, Applied Physics Letters, 2018, vol. 112, no. 6, art. no. 060401.

УДК 539.23

## Структурные свойства и морфология тонких пленок $\beta$ -Ga<sub>2</sub>O<sub>3</sub>, полученных на различных подложках золь-гель методом

М.К. Вронский<sup>1</sup>, А.Ю. Иванов<sup>1</sup>, Л.А. Сокура<sup>1,2</sup>, А.В. Кремлева<sup>1</sup>, Д.А. Бауман<sup>1</sup>

<sup>1</sup> Институт перспективных систем передачи данных Университета ИТМО, Кронверкский пр., д. 49, лит А, Санкт-Петербург, 197101, Россия

<sup>2</sup> ФТИ им. Иоффе РАН, ул. Политехническая, д. 26, Санкт-Петербург, 194021, Россия

**Аннотация.** В данной работе методом золь-гель были получены тонкие плёнки  $\beta$ -Ga<sub>2</sub>O<sub>3</sub> на подложках из сапфира и кварца, а также на буферных слоях Si-O. С помощью методов рентгеновской дифракции, сканирующей электронной микроскопии и оптической спектроскопии показано, что золь-гель методом могут быть получены плёнки  $\beta$ -Ga<sub>2</sub>O<sub>3</sub> с хорошими оптическими свойствами и кристаллическим качеством. Определенная по методу Тауца энергия оптической запрещенной зоны пленок варьировалась от 4,39 до 4,59 эВ.

**Ключевые слова:**  $\beta$ -Ga<sub>2</sub>O<sub>3</sub>; широкозонный полупроводник; рентгеновская дифрактометрия; тонкие плёнки; золь-гель